Molecular Recognition of Cytosine- and Guanine-Functionalized Nucleolipids in the Mixed Monolayers at the Air−Water Interface and Langmuir−Blodgett Films

Yuchun Wang, Xuezhong Du,* Wangen Miao, and Yingqiu Liang*

Key Laboratory of Mesoscopic Chemistry, Ministry of Education, and Department of Chemistry, Nanjing University, Nanjing 210093, P. R. China

Received: September 6, 2005; In Final Form: January 8, 2006

Molecular recognition of mixed nucleolipids of 1-(2-octadecyloxycarbonylethyl)cytosine and 7-(2-octadecyloxycarbonylethyl)guanine in the monolayers at the air−water interface and Langmuir−Blodgett (LB) films has been investigated in detail using surface pressure/potential−area isotherms, infrared reflection−absorption spectroscopy (IRRAS), and Fourier transform infrared (FTIR) transmission spectroscopy, respectively. Prior to molecular recognition, the cytosine moieties in the monolayer were hydrogen bonded with an almost flat-on orientation, the alkyl chains were uniaxially oriented with respect to the film normal, the guanine moieties in the monolayer were stacked probably through $\pi-\pi$ interaction with an end-on orientation, and the C−C−C planes of the alkyl chains were preferentially oriented parallel to the water surface. In the monolayer of equimolar mixture, molecular recognition between the cytosine and guanine moieties occurred together with the ring planes of base pairing and the C−C−C planes of the alkyl chains favorably oriented parallel to the water surface. The guanine moieties underwent an orientation change from an end-on mode before molecular recognition to a flat-on one after molecular recognition. The base pairing between the cytosine and guanine moieties in the monolayers was achieved since the N7-substituted guanine derivatives suppressed the formation of guanine tetramers. Both the IRRAS spectra of the monolayers and the FTIR spectra of the LB films presented the exact sites in the cytosine and guanine moieties for the formation of triple hydrogen bonds. The base pairing resulted in a change in molecular orientation and interaction, and the corresponding LB film exhibited a different phase transition behavior from a typical crystal transition for the cytosine-functionalized nucleolipids and an analogous glass transition for the guanine-functionalized nucleolipids. The thermal stability of the mixed LB film was improved in comparison to the LB films of pure components.

Introduction

Molecular recognition by means of multiple hydrogen bonds is of great importance in biological functions because the specific recognition of complementary bases in nucleic acids is the basis of their stable double-helix structure and the most efficient mechanism of accumulating, storing, and evolving genetic information.[1] Some derivatives of nucleotides, including nucleolipids, have been found to possess anticancer and antivirus properties.[2,3] Analysis and mimicry of the molecular recognition processes not only lead to a better understanding of biomembrane functions and processes but also can be helpful in the development of novel medicines and biosensors.[2,4]

Hydrogen bonding is usually suppressed or less effective for specific recognition in aqueous solution since the molecules are surrounded by bulk water;[5] as a result, base pairing of free nucleotides is not observed in water. Realization of effective hydrogen bonding in water is especially significant due to its relevance to biological recognition.[6] A few mimetic systems, such as micelles,[7−9] vesicles,[10] and monolayers at the air−water interface,[11−20] have been developed in the past decade to mimic molecular recognition of complementary nucleobases in aqueous systems. The organized nucleolipid monolayers at the air−water interface might act like a single nucleic acid strand, due to the hydrophobic interaction between the corresponding alkyl chains, to recognize their complementary bases in the subphase.

Most of the studies on molecular recognition of complementary hydrogen bonding in the monolayers at the air−water interface and Langmuir−Blodgett (LB) films are limited to nucleobase-like amphiphiles, such as melamine and barbituric acid derivatives,[6,21−24] and the studies about base pairing are focused on the adenine and uracil/thymine moieties in nucluolipids.[11−17] Moreover, much emphasis is placed upon the interaction between the host monolayers and guest components in the subphase, and no attention is attracted to the competition of the host−host interactions with the host−guest ones. Our recent studies indicated that the monolayer of cytosine-functionalized nucleolipids on the aqueous guanosine subphase underwent an orientation change not only in base moiety but also in alkyl chain in comparison to the monolayer on pure water,[19,20] and these revealed the interconversion of hydrogen bonds between adjacent cytosine moieties and between cytosine and guanosine base pairs in the courses of molecular recognition and the phase transition behaviors of the corresponding LB films.[19,20]

To date, few studies on molecular recognition of cytosine and guanine base pairing at the interface have been reported,[18−20] especially for guanine-functionalized nucleolipids. Among all of the nucleobases, guanine possesses a unique ability to self-organize via cyclic interactions to form quartets of a regular, ordered structure by hydrogen bonds between the sites N1 and N2 as donors and O6 and N7 as acceptors,[25,26] which is the probable reason for molecular recognition of cytosine and

* To whom correspondence should be addressed. E-mail: xzdu@nju.edu.cn (X.D.). Fax: 86-25-83317761.

10.1021/jp055046z CCC: $33.50
Published on Web 02/17/2006

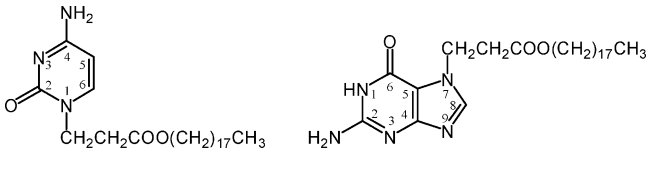

1 **2**

Figure 1. Chemical structures of nucleolipids 1-(2-octadecyloxycarbonylethyl)cytosine (**1**) and 7-(2-octadecyloxycarbonylethyl)guanine (**2**).

guanine moieties being unavailable in mimetic systems. Herein, nucleolipids 1-(2-octadecyloxycarbonylethyl)cytosine (**1**) and 7-(2-octadecyloxycarbonylethyl)guanine (**2**) were synthesized, the chemical structures of which are shown in Figure 1. This meant that the stable planar tetramers via quadruple hydrogen bonding each guanine might be suppressed because nucleolipid **2** was an N7-substituted guanine derivative.

To have a full understanding of the mimetic molecular recognition in an aqueous environment, which is close to that of the nucleic acids in biological systems, an in-situ characterization technique is necessary for studies of molecular recognition on the molecular level. Infrared reflection−absorption spectroscopy (IRRAS) has been a leading structural method for the in-situ characterization of the monolayers at the air−water interface.[27,28] The IRRAS technique can provide abundant information on molecular interaction not only between the hydrophilic headgroups but also between the hydrophobic chains. However, few studies have been so far devoted to the characterization of the mimetic molecular recognition via hydrogen bonds.[20,21] Furthermore, studies on the phase transition properties of the corresponding LB films prior to and after molecular recognition can give a deeper understanding of the effect of molecular recognition between the headgroups on the interaction between the alkyl chains.

In this paper, molecular recognition of nucleolipids **1** and **2** in the mixed monolayers at the air−water interface and in LB films has been investigated in detail using surface pressure/potential−area isotherms, an in-situ IRRAS technique, and ex-situ FTIR transmission spectroscopy. Completely different base orientation and intermolecular interaction in the mixed monolayers were presented in comparison to those in the monolayers on the complementary base-containing subphase,[19,20] which will give a guide to the molecular design of amphiphiles for functional supramolecular architecture.

Experimental Section

Nucleolipid Preparation. The synthesis of nucleolipid **1** was recently reported in detail.[19] The synthesis of nucleolipid **2** is described in the following. A solution of 7-(2-carboxylethyl)-guanine (223 mg, 1 mmol), which was prepared using the method in the literature,[29] and KOH powder (56 mg, 1 mmol) in dry DMSO (10 mL) was stirred at 60 °C and kept at that temperature for 4 h. Octadecyl methanesufonate (348 mg, 1 mmol) was then added to the solution. The reaction mixture was further stirred for 16 h. After cooling, the mixture was poured into 200 mL of water. White precipitate was washed with water and dried in a vacuum over anhydrous P_2O_5. The white solid was purified via a silica gel column, first eluted with chloroform and then with methanol/chloroform (2/23, v/v), to give 330 mg of **2** in 69% yield. ^{1}H NMR ($CDCl_3$): 7.63 (s, 1H, H-8); 6.33 (broad, 2H, NH_2); 4.24 (t, 2H, H(1′)); 4.01 (t, 2H, H(2′)); 2.85 (t, 2H, CH_2(2)); 1.75 (m, 2H, CH_2(3)); 1.17 (m, 28H, CH_2(4−17)); 0.80 (t, 3H, CH_3(18)). Anal. Calcd for $C_{26}H_{45}N_5O_3$: C, 65.65; H, 9.54; N, 14.72. Found: C, 65.80; H, 9.77; N, 14.71.

Nucleolipids **1** and **2** were prepared as 1 mmol/L solutions in chloroform, respectively, and stored at 4 °C prior to use. Their equimolar mixture was prepared volumetrically from the stock solutions. The equimolar mixture was chosen here mainly on the basis of the well-known base pairing in the nucleic acid double-helix structures.[30]

Isotherms and LB Film Preparation. The monolayer spreading was performed on a Nima 611 Langmuir−Blodgett trough (England). The maximum available surface area was 30 × 10 cm^2 and could be varied continuously by moving two Teflon barriers. Water used for the subphase (resistivity 18.2 MΩ cm) was double-distilled after a deionized Milli-Q exchange. A Wilhelmy plate (filter paper) was used as the surface pressure sensor with an accuracy of ±0.1 mN/m and situated in the middle of the trough. Surface potential measurements were performed on a Trek electrometer. A vibrating electrode was placed at about 2 mm above the air−water interface, and a stainless steel plate as the reference electrode was immersed in the subphase. Monolayers were obtained by spreading the desired volumes of chloroform solutions in the concentration 1 mmol/L on the surface of pure water. The subphase temperature was kept at 22 °C. After spreading, 15 min was allowed for solvent evaporation, and then, the monolayers were compressed at a rate of 8 mm/min to record isotherms. For the preparation of LB films, the monolayers were first compressed to the surface pressure of 20 mN/m and, then, 30 min was allowed for the monolayer to reach equilibrium. Nine-layer LB films were transferred onto CaF_2 substrates by the vertical method at a dipping rate of 2.0 mm/min. The mixture monolayers could be transferred in the *Y* type, but the monolayers of individual components were only deposited in the upstrokes (*Z* type).

IRRAS Spectrum Measurements. IRRAS spectra of the nucleolipid monolayers at the air−water interface were recorded on an Equinox 55 FTIR spectrometer equipped with a Bruker XA-511 external reflection attachment containing a shuttle Langmuir trough using a mercury-cadmium-telluride (MCT) detector and a KRS-5 polarizer. The rate of shuttle movement was 32 cm/min. A faster speed would disturb the monolayers, while a slower one would prolong the time interval between the sample and reference measurements, which resulted in a strong interference of vapor. The temperature was kept at 22 °C. The film-forming molecules were spread from chloroform solutions of the desired volumes. After the chloroform was evaporated, the measurement system was enclosed for humidity equilibrium for 4 h prior to compression. The monolayers were then compressed discontinuously to the preset surface pressures, and then, 30 min was allowed for monolayer relaxation before spectrum acquisition. The IRRAS data were always collected with a resolution of 8 cm^{-1} by coaddition of 1024 scans at the fixed area after the desired surface pressure was reached, and IRRAS spectra of high signal-to-noise ratio could be obtained by carefully controlling the experimental conditions. The external reflection−absorption spectrum of pure water was used as a reference. A time delay of 30 s was allowed for the monolayer to reach equilibrium between trough movement and data collection. During the IR data acquisition, no obvious relaxation (≤0.2 mN/m) for the monolayers at different surface pressures (0−20 mN/m) was observed. The angle of incidence dependent measurements were carried out for the monolayers at a surface pressure of 20 mN/m, and the surface pressure drops throughout the measurements were in the range 1.3−3.5 mN/m dependent on monolayers. All of the IRRAS spectra were used without smoothing or correction.

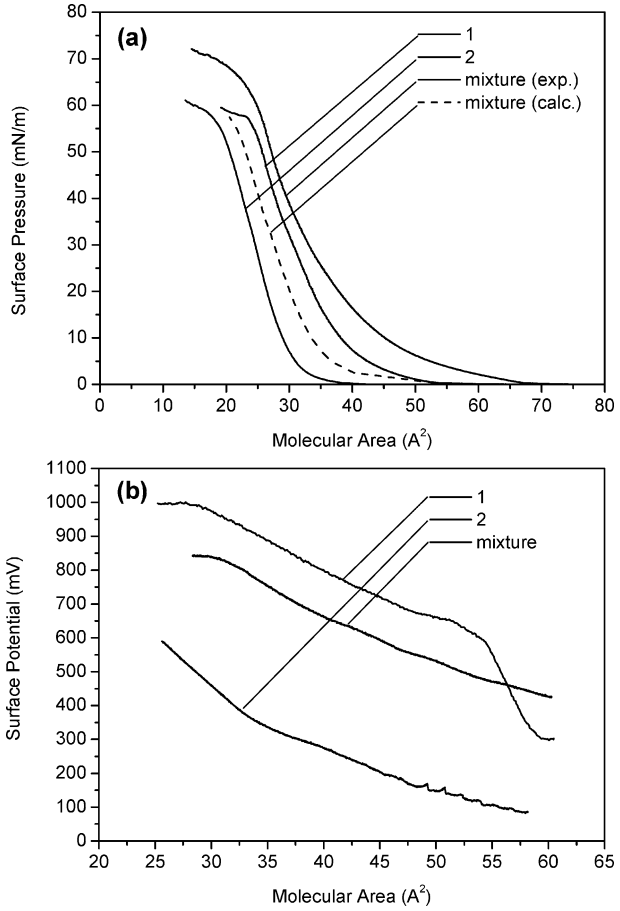

Figure 2. Isotherms of the monolayers of nucleolipids **1**, **2**, and their equimolar mixture at the air−water interface on pure water with the compression rate 8 mm/min at 22 °C, together with an ideal mixing behavior for comparison: (a) surface pressure−area isotherm; (b) surface potential−area isotherm.

FTIR Transmission Measurements. FTIR transmission spectra were recorded on a Bruker IFS 66V spectrometer with a deuterated triglycine sulfate (DTGS) detector. Typically, 1000 scans were collected to obtain a satisfactory signal-to-noise ratio with a resolution of 4 cm^{-1}. For the IR spectra of LB films at the elevated temperatures, a CaF_2 substrate with the deposited LB film was mounted into a heating cell and temperature control was achieved with a P/N 21.500 automatic temperature controller (Graseby Specac Inc.) through a copper−constantan thermocouple with an accuracy of ±1 °C. After the temperature was raised to the preset value, 15 min was allowed for thermal equilibrium to be reached. The variable-temperature spectra were collected for 500 scans at a resolution of 4 cm^{-1}.

Results and Discussion

Isotherms of the Monolayers at the Air−Water Interface. Figure 2a shows surface pressure−area (π−A) isotherms of the monolayers of **1**, **2**, and their equimolar mixture on pure water. Nucleolipid **1** formed a stable monolayer with a transition from a liquid-expanded phase to a liquid-condensed one. The collapse pressure and limiting area were estimated to be 57 mN/m and 36 Å^2 per molecule, respectively. The limiting area was obviously greater than the cross-sectional area of a hydrocarbon chain (ca. 20 Å^2), indicating that the limiting area was predominantly determined by cytosine moieties. The crystal structure of cytosine is determined to be orthohombic with the unit cell dimensions $a = 13.041$, $b = 9.494$, and $c = 3.815$ Å containing four molecules, and the molecules are tilted about 27.5° from parallel to the *ab* plane.[31] On the basis of the cytosine dimensions, each cytosine occupied an area of $(13.041 \times 9.494)/(4 \times \cos 27.5)$ Å^2 = 35 Å^2 when lying flat on a surface. Taking the limiting area and cytosine dimensions into account, it was obvious that the planes of the cytosine moieties almost adopted a parallel (flat-on) orientation to the water surface. This would be favorable to the formation of intermolecular hydrogen bonds between the adjacent cytosine moieties. Nucleolipid **2** formed a condensed monolayer with a collapse pressure of about 55 mN/m and a limiting molecular area of 30 Å^2 per molecule. Tao and Shi studied monolayer guanine on graphite using both scanning tunneling microscopy (STM) and atomic force microscopy (AFM) and obtained two sets of lattice constants of $a = 8.5$ Å, $b = 11.5$ Å, and $\gamma = 90 \pm 2°$ (two molecules per unit cell from AFM) and $a = 8.5 \pm 0.5$ Å, $b = 33 \pm 1.5$ Å, and $\gamma = 90 \pm 3°$ (six molecules per unit cell from STM).[32] On the basis of the guanine dimensions, each guanine could be estimated to occupy an area of 47 Å^2 when lying flat on the graphite substrate. Obviously, the guanine moieties in the monolayer preferentially took an end-on orientation (a tilt angle far away from the water surface). It has been observed that nucleobases tend to stack into polymeric aggregates in bulk solution.[33] The stacked structures are found to be preserved for guanine and adenine on Au(111),[34] while they are lost on graphite due to strong guanine−graphite and adenine−graphite interactions which overwhelm the base stacking forces.[32] It seemed that the guanine moieties in the monolayer were stacked probably through π−π interaction. Compared with nucleolipids **1** and **2**, their equimolar mixture displayed an expanded behavior with a slight increase of the collapse pressure, which was considerably different from their ideal mixing according to the equation provided by Gaines.[35] The behavior indicated that the molecular recognition between the complementary base moieties took place at the air−water interface. The limiting area extrapolated from the isotherm of the mixed monolayer was 39 Å^2 per molecule, greater than the limiting area (34 Å^2 per molecule) estimated from the theoretical isotherm. This suggested that the expansion of the monolayer originated from a change in the guanine orientation from the end-on mode to a flat-on one, which was favorable to the formation of hydrogen bonds between the two complementary base moieties within the monolayer.

The surface potential−area isotherms of the monolayers of **1**, **2**, and their equimolar mixture on pure water are presented in Figure 2b. The surface potentials were nonzero even at large molecular areas, suggesting that large aggregates were formed immediately after spreading.[36] However, the surface potential of **1** was much higher than that of **2**, indicating that the cytosine−cytosine interaction (intermolecular hydrogen bonds) was stronger than the guanine−guanine interaction (π−π stacking). Obviously, the surface potential of the mixture was higher than either of the two individual components at the large molecular areas, implying the occurrence of strong intermolecular hydrogen bonding interaction between the cytosine and guanine moieties. Upon compression, no "jump" in the surface potential−area isotherm was observed in the mixed monolayer, and the surface potential rose steadily. These features indicated that the mixed monolayer was homogeneous (miscible). The change of surface potential for the mixed monolayer was similar to that for the monolayer of **2**, suggesting that the chain packing and orientation in the mixed monolayer might be analogous to those in the monolayer of **2**.

All of the monolayers of the two individual components and their mixture showed a hysteresis effect during the compres-

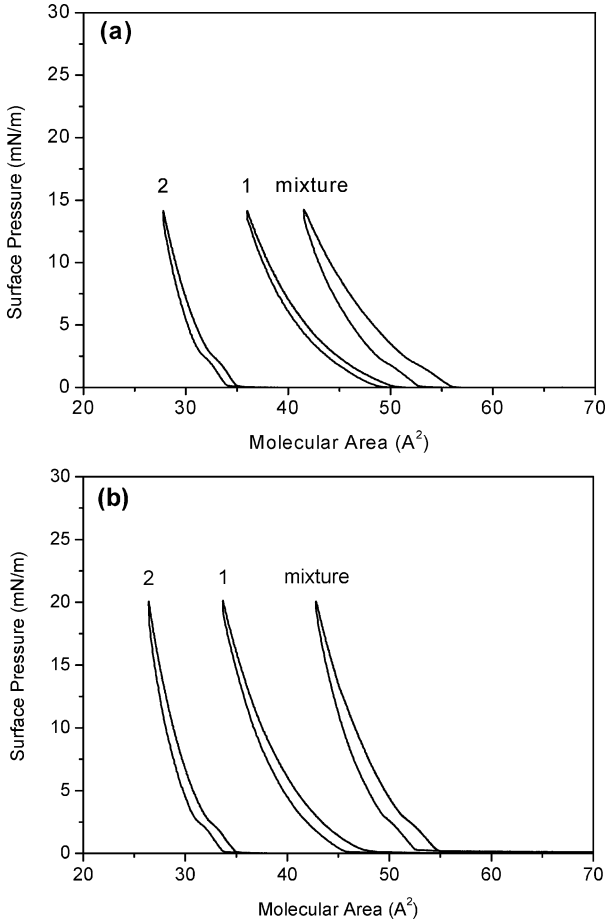

Figure 3. Compression−expansion cycles of the surface pressure−area isotherms of the monolayers on pure water with the rate 8 mm/min at 22 °C: (a) 14 mN/m; (b) 20 mN/m.

sion−expansion cycles at surface pressures of 14 and 20 mN/m investigated (see Figure 3), due to intermolecular hydrogen bonding or $\pi-\pi$ interactions between the base moieties. However, the mixed monolayer displayed higher a hysteresis effect than either of the individual components, which indicated that the mixed monolayer was miscible. This meant that strong intermolecular hydrogen bonding interactions were formed between the cytosine and guanine moieties.

IRRAS Spectra of the Monolayers at the Air−Water Interface. Figure 4a shows p-polarized IRRAS spectra of the monolayers of nucleolipid **1** on pure water at different surface pressures. In the vicinity of 0 mN/m, the two bands at 2923 and 2853 cm^{-1} were assigned to the antisymmetric and symmetric CH_2 stretching modes [$\nu_a(CH_2)$ and $\nu_s(CH_2)$] of hydrocarbon chains, respectively. It is known that the $\nu_a(CH_2)$ and $\nu_s(CH_2)$ frequencies are sensitive to the conformation order of alkyl chains.[37,38] Lower wavenumbers are characteristic of preferential all-trans conformers in highly ordered chains, while the number of gauche conformers increases with the frequency and width of the bands. The vibrational frequencies at 2923 and 2853 cm^{-1} around 0 mN/m indicated that the alkyl chains were disordered with the population of gauche conformers. Upon an increase in surface pressure, the two bands were obviously intensified and shifted down to 2920 and 2851 cm^{-1}, respectively, indicative of an increase of chain order. The IRRAS spectral changes were in agreement with the isotherm of the monolayer including a transition from a liquid-expanded phase to a liquid-condensed one. A single band at 1728 cm^{-1} was assigned to the C═O stretching vibration [ν(C═O)] of ester groups incorporated in the alkyl chains. The band at 1655 cm^{-1}

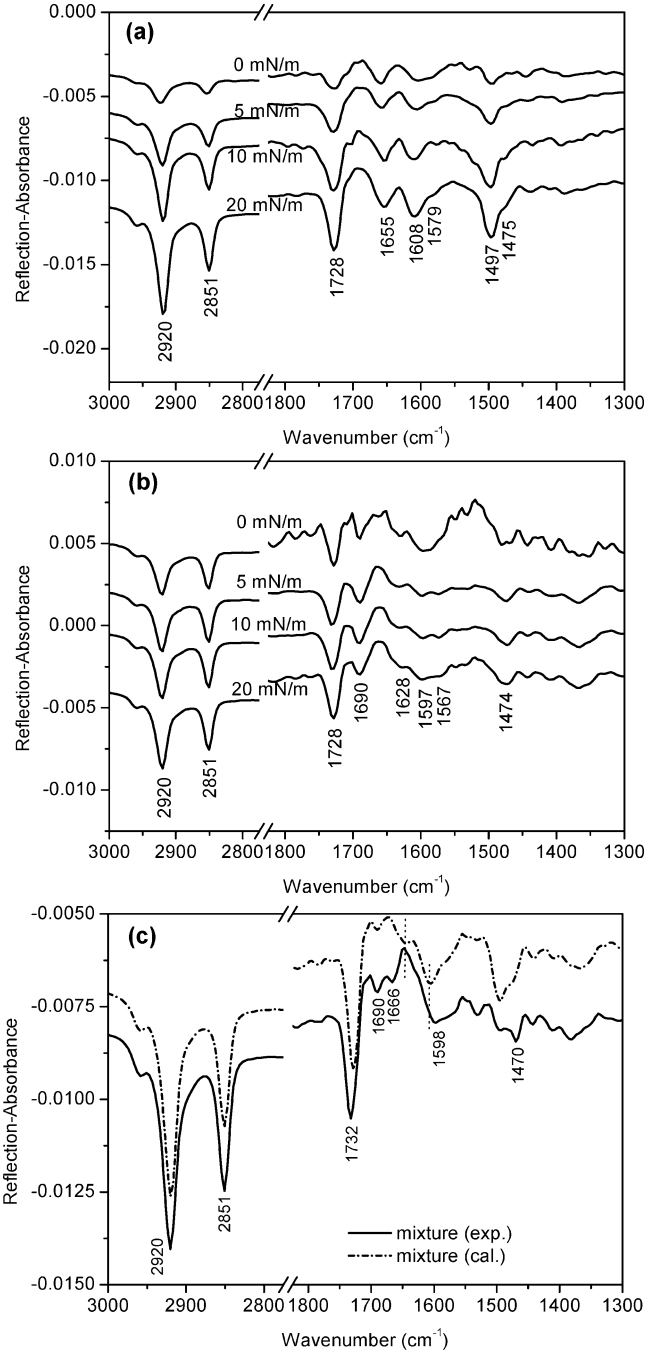

Figure 4. IRRAS spectra of the monolayers of nucleolipids (a) **1** and (b) **2** at various surface pressures, and (c) their equimolar mixture at the air−water interface at a surface pressure of 20 mN/m in comparison to the IRRAS spectrum of the calculated equimolar mixture on the basis of IRRAS spectra of **1** and **2** at 20 mN/m: angle of incidence, 30°; p-polarization; 22 °C.

originated from several superimposed modes, creating a broad peak where the C2═O stretching mode appeared to be the main component.[39] The frequency of this mode suggested that the C2═O groups were involved in hydrogen bonding to neighboring cytosine moieties, because free C═O groups (matrix-isolated) were expected to be near 1710−1720 cm^{-1}.[40] The band around 1608 cm^{-1} was due to the coupled stretching vibrations of the C5═C6 and C4═N3 bonds in the cytosine moieties.[41] The shoulder around 1579 cm^{-1} and the band at 1497 cm^{-1} were attributed to the ring quadrant stretching vibrations.[41−43] A shoulder around 1475 cm^{-1} overlapped with the 1497 cm^{-1} band and was mainly assigned to the CH_2 scissoring vibration

[$\delta(CH_2)$] of the alkyl chains as well as the ring stretching vibrations.[41,42,44] As seen from the figure, the two bands at 1728 (the ester incorporated in the chains) and 1497 cm^{-1} (superimposed by the $\delta(CH_2)$ peak) grew in intensity with surface pressure in a similar trend to the $\nu_a(CH_2)$ and $\nu_s(CH_2)$ bands, which was relevant to a change in chain conformation and orientation with surface pressure, whereas the two bands at 1655 and 1608 cm^{-1} due to the stretching vibrations of the cytosine moieties showed a relatively slow increase in intensity with surface pressure. This implied that the orientation of the cytosine moieties was almost independent of surface pressure, which was consistent with the flat-on orientation of the cytosine moieties in the monolayers inferred from the corresponding isotherm.

Figure 4b shows p-polarized IRRAS spectra of the monolayers of nucleolipid **2** on pure water at different surface pressures. In the range of 0−20 mN/m, the $\nu_a(CH_2)$ and $\nu_s(CH_2)$ bands appeared at 2920 and 2851 cm^{-1}, respectively. The intensities of the two bands increase gradually with surface pressure, but their frequencies were independent of surface pressure. The spectral features were in accordance with the behavior of the liquid-condensed monolayer. The single band at 1728 cm^{-1} was due to the C═O stretching vibration of ester groups incorporated in the alkyl chains. Similarly, the band increased in intensity in an almost identical trend to the $\nu_a(CH_2)$ and $\nu_s(CH_2)$ bands. A band at 1690 cm^{-1} was assigned to the mixed modes of the C6═O stretching and NH_2 scissoring vibrations in the guanine moieties;[39,41,45] however, the band underwent a decrease in intensity instead of an increase with surface pressure. The spectral changes suggested that the guanine moieties took an end-on orientation and the tilt angle of the base planes from the water surface increased with surface pressure, which was in good agreement with the analysis of the corresponding $\pi-A$ isotherm. A band around 1628 cm^{-1} was due to the C═C and C═N stretching modes in the guanine moieties[41,45] together with the NH_2 scissoring vibration.[39] The bands at 1597 and 1567 cm^{-1} were attributed to the ring quadrant stretching vibrations,[41−43] and the band around 1474 cm^{-1} was mainly due to the $\delta(CH_2)$ mode.[46]

Figure 4c shows the IRRAS spectrum of the monolayer of the equimolar mixture of nucleolipids **1** and **2** at 20 mN/m in comparison with the estimated spectrum from the IRRAS spectra of **1** and **2**. A new peak at 1666 cm^{-1} was clearly observed, which was a result of molecular recognition between the cytosine and guanine moieties via hydrogen bonds. In the case of **1**, the band at 1655 cm^{-1} was due to the mixed modes of the C2═O stretching and NH_2 scissoring vibrations in the cytosine moieties.[39,41,42] In the case of **2**, the band at 1690 cm^{-1} was due to the mixed modes of the C6═O stretching and the NH_2 scissoring vibrations in the guanine moieties.[41,45] It was obvious that the new band at 1666 cm^{-1} was predominantly due to the mixed modes of the NH_2 bending vibration of the cytosine moieties and the C6═O stretching vibration of the guanine moieties. The band at 1690 cm^{-1} in the case of the equimolar mixture was mainly due to the NH_2 scissoring vibration in the guanine moieties, and the peak from the C2═O stretching mode in the cytosine moieties could not be distinguished probably due to the positive $\delta(H_2O)$ band of subphase water. These spectral changes indicated that molecular recognition took place between the cytosine and guanine moieties via the hydrogen bonds $C2^C{=}O\cdots H{-}N^G{-}H$ and $H{-}N^C{-}H\cdots O{=}C6^G$. The band due to the coupled modes of the C═N and C═C stretching vibrations in the two base moieties[41] took a downshift to 1598 cm^{-1}, which suggested that the N3 sites in the cytosine moieties were involved in hydrogen bonding to the guanine moieties via $N3^C\cdots H{-}N1^G$.

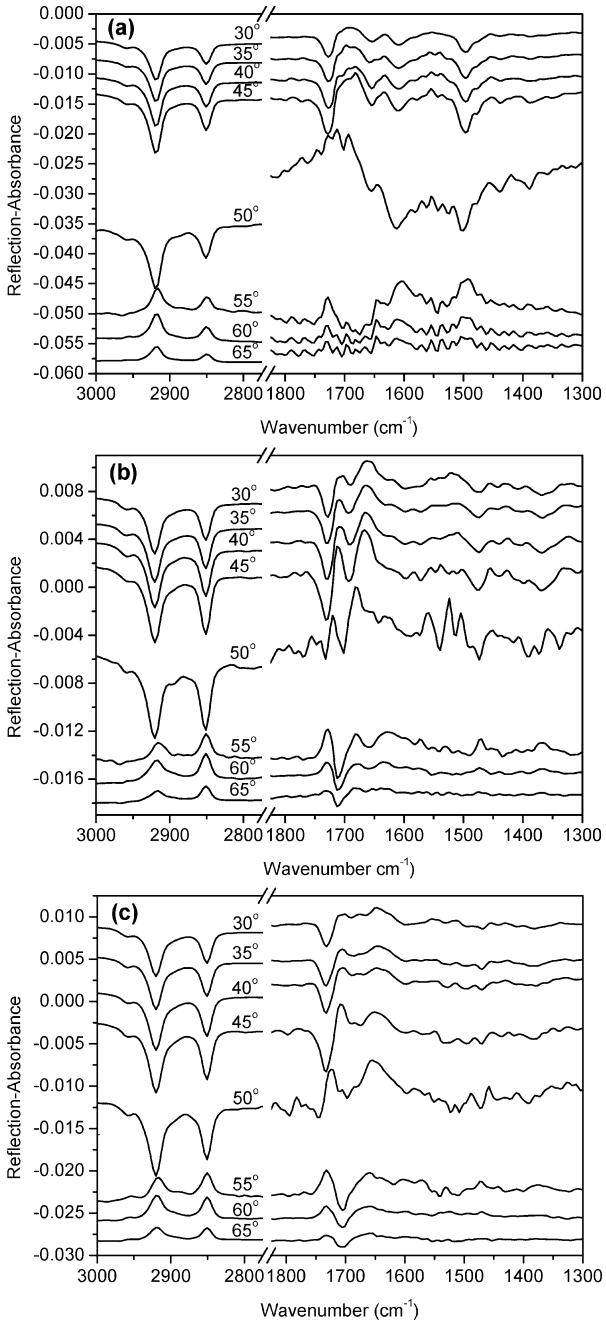

Figure 5. IRRAS spectra of the monolayers of nucleolipids (a) **1**, (b) **2**, and (c) their equimolar mixture at the air−water interface at various angles of incidence: p-polarization; 22 °C.

Figure 5 shows p-polarized IRRAS spectra of the monolayers of nucleolipids **1**, **2**, and their equimolar mixture at various angles of incidence, respectively. For p-polarized radiation, which is polarized parallel to the plane of incidence, the bands are initially negative and their intensities increase with increasing angle of incidence and reach a maximum; then, a minimum in the reflectivity is found at the Brewster angle (see parts a−c of Figure 5). The exact position of the Brewster angle φ depends on the wavelength of light and the optical properties of the substrate. For the air−water interface, the Brewster angle can be estimated by calculating $\tan \varphi = n_{water}$, where n_{water} is the real part of the H_2O refractive index at a given wavenumber [$\varphi = 54.5°$ for the $\nu_a(CH_2)$ band at 2920 cm^{-1} ($n_2 = 1.402$),[47] and $\varphi = 54.2°$ for the $\nu_s(CH_2)$ band at 2851 cm^{-1} ($n_2 = 1.386$)[47]].

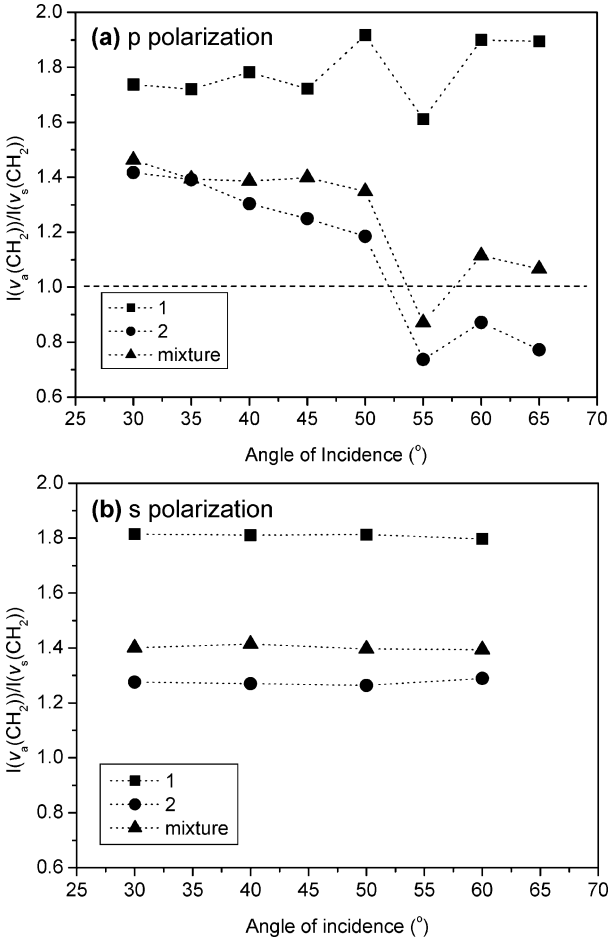

Figure 6. Ratio of band intensity [$\nu_a(CH_2)/\nu_s(CH_2)$] of IRRAS spectra of the monolayers of nucleolipids **1**, **2**, and their equimolar mixture at the air−water interface as a function of the angle of incidence: (a) p-polarization; (b) s-polarization.

Beyond the Brewster angle, the bands become positive and their intensities decrease upon further increase of the incident angle. For s-polarized radiation, which is polarized perpendicular to the plane of incidence, the bands are always negative and the intensity decreases with increasing angle of incidence (s-polarized spectra are shown in the Supporting Information). For the cytosine and guanine moieties, the majority of vibrational peaks were generally of mixed character;[39] therefore, it did not seem to be easy to give a theoretical estimation of the base orientation. The calculation of chain orientation developed by Gericke[28] on the basis of Kuzmin and Michailov's model[48] was suited for the uniaxial distribution of hydrocarbon chains with all-trans conformations.[28] The chain orientation in the monolayer of **1** was estimated using the method, and the alkyl chains were oriented at a tilt angle of 20° with respect to the surface normal.[20] For the p-polarized spectra of the monolayer of **2** (part b of Figure 5), the ratio of the $\nu_a(CH_2)$ band intensity to the $\nu_s(CH_2)$ one [$\nu_a(CH_2)/\nu_s(CH_2)$] showed a different change from that for the monolayer of **1** (see part a of Figure 6). Below the Brewster angle, the extent of the increase in the $\nu_s(CH_2)$ band intensity was more than that in the $\nu_a(CH_2)$ one in the case of **2**, so that the ratio was reduced with increasing angle of incidence in contrast to a roughly unchanged value centered around 1.7−1.8 in the case of **1**. Beyond the Brewster angle, the two bands were positive-oriented, but the $\nu_a(CH_2)$ intensities were considerably reduced in comparison to the $\nu_s(CH_2)$ ones. For s-polarization, the intensity ratio of the two bands was greater than 1 and remained constant with increasing angle of incidence for the monolayers investigated (part b of Figure 6).

It is known that both methylene transition moment directions are perpendicular to the alkyl chains, with the $\nu_s(CH_2)$ transition moment being oriented along the bisector of the methylene H−C−H bond angle, while the $\nu_a(CH_2)$ transition moment is perpendicular to this. For s-polarization, a methylene stretching band intensity will become maximal, when all transition moments are oriented horizontally, i.e., when the alkyl chains are perpendicular to the water surface. For s-polarization of the IR beam, bands are always negative and the intensity decreases with increasing angle of incidence. For p-polarization of the IR beam, the bands are initially negative and the band intensity increases with increasing angle of incidence until the Brewster angle is reached. Beyond the Brewster angle, the band becomes positive and the band intensity decreases upon further increase of the angle of incidence. For a vibration with a transition moment along the surface normal (perpendicular to the water surface), the situation is reversed: for incident angles smaller than the Brewster angle, a positive band will be observed, while for larger angles a negative band will be found.[49] The spectral changes in part b of Figure 5 indicated that the C−C−C planes of the alkyl chains were preferentially oriented parallel to the water surface, together with the $\nu_s(CH_2)$ transition moments parallel to the water surface and the $\nu_a(CH_2)$ ones perpendicular to the water surface more or less. The apparent reduction in the $\nu_a(CH_2)$ intensity resulted from the opposite signs of the bands with the directional transition moments oriented along the surface normal.[50] It was obvious that the preferential orientation of the alkyl chains was closely related to the end-on orientation of the guanine moieties.

Figure 5c shows p-polarized IRRAS spectra of the monolayer of the equimolar mixture at various angles of incidence, and the intensity ratio $\nu_a(CH_2)/\nu_s(CH_2)$ as a function of incident angle is also presented in Figure 6. The case for the equimolar mixture was intermediate between nucleolipids **1** and **2**. The intensity ratios $\nu_a(CH_2)/\nu_s(CH_2)$ almost remained approximately 1.4 below the Brewster angle. Beyond the Brewster angle, the two $\nu_a(CH_2)$ and $\nu_s(CH_2)$ bands became positive-oriented and the ratios $\nu_a(CH_2)/\nu_s(CH_2)$ were reduced to be even smaller than 1. This indicated that the C−C−C planes of the alkyl chains in the mixed monolayer were preferentially oriented parallel to the water surface to a certain extent.

FTIR Spectra of LB Films. Figure 7a shows FTIR transmission spectra of nine-layer LB films of **1**, **2**, and their equimolar mixture transferred from pure water. The two strong bands around 2917−2918 and 2849−2850 cm^{-1} were due to the $\nu_a(CH_2)$ and $\nu_s(CH_2)$ vibrations, respectively. The frequency positions were characteristic of highly ordered alkyl chains with almost all-trans conformations. In the spectrum of **1**, the bands around 3358 and 3121 cm^{-1} were assigned to the antisymmetric and symmetric NH_2 stretching vibration [$\nu_a(NH_2)$ and $\nu_s(NH_2)$] in the cytosine moieties.[41,42] The single band at 1731 cm^{-1} was due to the C═O stretching vibration of the ester groups incorporated in the chains. The corresponding second derivative spectrum shows that the broad band around 1660 cm^{-1} was composed of the two components at 1674 and 1660 cm^{-1}. The former was probably assigned to the NH_2 bending mode in the cytosine moieties,[21,22,39] and the latter, to the C2═O stretching mode.[39,41,42,44] The band positions of the $\nu(NH_2)$ and ν(C2═O) modes suggested that the cytosine moieties in the monolayers were involved in the intermolecular hydrogen bonds. The doublet peak at 1630 and 1620 cm^{-1} was due to the coupled vibrations of the C5═C6 and C4═N3 bonds in the cytosine

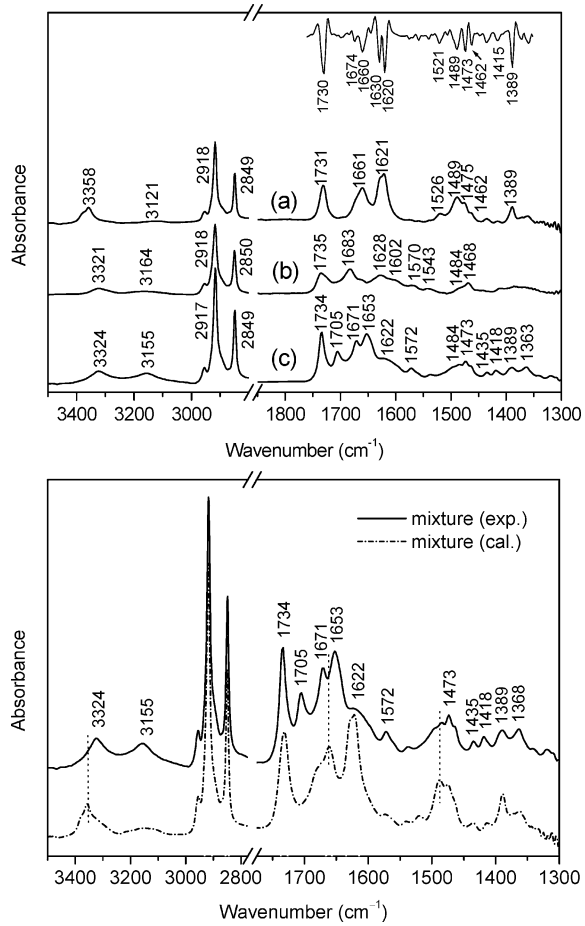

Figure 7. FTIR transmission spectra of nine-layer LB films of nucleolipids (a) **1**, (b) **2**, and (c) their equimolar mixture transferred from pure water as well as the second derivative spectrum of **1** (top) and the comparison of FTIR spectra of the LB films of the experimental and calculated equimolar mixtures (bottom).

rings.[41] The 1518 and 1489 cm^{-1} peaks were attributed to the ring quadrant stretching vibrations,[41−43] and the band at 1389 cm^{-1} was due to the ring semicycle stretching vibration mixed with the C═C−H deformation.[21,41−43] As seen from the spectrum, most of the vibrational bands relevant to the cytosine moieties displayed strong intensities, which indicated that the planes of the cytosine moieties preferentially took a flat-on orientation on the substrate. The doublet peak around 1473 and 1462 cm^{-1} (see the second derivative spectrum) was assigned to the $\delta(CH_2)$ scissoring mode as well as the ring stretching vibrations.[41,42,44] It is well-known that the $\delta(CH_2)$ vibration mode is extremely sensitive to the interaction between hydrocarbon chains.[46,51] The appearance of the $\delta(CH_2)$ splitting band is indicative of an orthorhombic subcell packing where the C−C−C planes of adjacent hydrocarbon chains are oriented at about 90° to each other.[52,53] It is reported that the crystal structure of cytosine is orthorhombic.[31] Obviously, the chain stacking was related to the packing structure of the nucleobase moieties.

In the spectrum of **2**, the broad peaks around 3321 and 3165 cm^{-1} were assigned to the $\nu_a(NH_2)$ and $\nu_s(NH_2)$ modes in the guanine moieties, respectively, mixed with the N1−H stretching vibration. Similarly, the band at 1735 cm^{-1} was due to the C═O stretching vibration in the ester groups, the broad band centered at 1683 cm^{-1} was attributed to the mixed modes of the C6═O stretch and the NH_2 deformation in the guanine bases.[41,45] A series of wide peaks in the region 1628−1484 cm^{-1} were due to the C═C, C═N, and ring quadrant stretching vibration.[41,45] As seen from the spectrum, the relative intensities of the vibrational bands relevant to the guanine moieties were weak, suggesting that the guanine moieties adopted an end-on orientation far away from the substrate surface.

The FTIR spectrum of the LB film of the equimolar mixture of **1** and **2** was obviously different from that of the estimated ideal mixing (the bottom panel of Figure 7). The $\nu_a(NH_2)$ stretching band was shifted down to 3324 cm^{-1}, indicating that molecular recognition between the cytosine and guanine moieties occurred through the intermolecular hydrogen bonds. The $\nu_s(NH_2)$ band at 3155 cm^{-1} was observed to increase in intensity, suggesting that the planes of the cytosine and guanine base pairing took a preferential orientation parallel to the substrate. This meant that the guanine moieties underwent a change in orientation from an end-on mode before molecular recognition to a flat-on one after molecular recognition. The orientation change was different from that for the monolayer of **1** on an aqueous guanosine solution, where the cytosine moieties took a change from a flat-on orientation before molecular recognition to an end-on one after molecular recognition.[20] It is known that the formation of hydrogen bonds gives rise to a lower wavenumber shift for stretching modes and a higher wavenumber shift for bending modes.[21] In the region 1750−1450 cm^{-1}, a new peak at 1705 cm^{-1} was clearly detected, which could be attributed to the NH_2 bending mode after molecular recognition. The $\delta(NH_2)$ frequency was increased from the component at 1674 cm^{-1} for the cytosine moieties and the component around 1683 cm^{-1} for the guanine moieties. The two bands at 1671 and 1653 cm^{-1} were assigned to the C6═O stretching vibration in the guanine moieties and the C2═O stretching mode in the cytosine moieties, respectively, because the corresponding C═O stretching band should be observed to shift to lower frequencies. It was obvious that the hydrogen bonds $C2^C{=}O\cdots H{-}N^G{-}H$ and $H{-}N^C{-}H\cdots O{=}C6^G$ were formed between the complementary bases cytosine and guanine. The band around 1620 cm^{-1}, primarily due to the C4═N3 stretching vibration in the cytosine moieties and the C═N stretching vibration in the guanine moieties coupled with the C═C stretching modes,[41] was substantially reduced in intensity into a shoulder. The spectral changes suggest that the N3 sites in the cytosine moieties were involved in hydrogen bonding to the guanine moieties via $N3^C\cdots H{-}N1^G$. The bands around 1572 and 1489 cm^{-1} underwent an increase and a decrease in intensity, respectively, and the band at 1390 cm^{-1} due to the semicircle ring stretching vibration was considerably diminished in intensity. Since the nitrogen atoms from the base rings participated in the formation of hydrogen bonds, some of the ring stretching vibrations were also affected by the hydrogen bonds to become inactive or active so that the corresponding ring stretching bands were weakened or intensified.[21] All of these spectral features demonstrated the occurrence of specific molecular recognition by means of triple hydrogen bonds between the cytosine moieties at the positions C2═O, N3, and NH_2 and the complementary guanine bases at the positions NH_2, N1−H, and C6═O. The exact sites of the triple hydrogen bonding interaction were clearly confirmed. In combination with the above studies, the orientation of the base moieties and alkyl chains in the monolayers of the two individual components and their mixture as well as the base pairing via hydrogen bonds were schematically illustrated in Figure 8.

Phase Transition Behaviors of LB Films. The phase transition behaviors of LB films correlate well with the interchain interaction and molecular structure of the film-forming molecules. It is well-known that the $\nu_a(CH_2)$ frequency

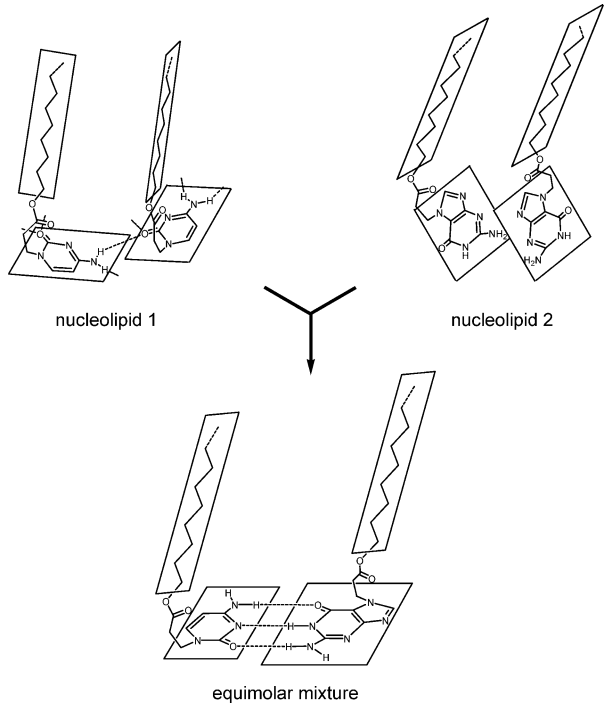

Figure 8. Schematic illustration of the orientation of base moieties and alkyl chains in the monolayers of nucleolipids **1**, **2**, and their mixture together with base pairing through hydrogen bonds.

is very sensitive to the conformation of hydrocarbon chains.[37,38] FTIR spectroscopy is a powerful tool to monitor precisely subtle changes in chain conformation.

Figure 9 shows variable-temperature FTIR spectra of nine-layer LB films of **1**, **2**, and their equimolar mixture deposited from pure water in the region 3000−2800 cm^{-1}. The corresponding temperature-dependent $\nu_a(CH_2)$ frequencies are presented in Figure 10. At 30 °C, the alkyl chains in the LB film of **2** were a little disordered with a small fraction of gauche conformations, while the chains in the films of **1** and the equimolar mixture were highly ordered with almost all-trans conformations, particularly for the equimolar mixture. This indicated that the molecular recognition between the complementary base moieties caused an increase of chain order. As the temperature ramp continued, the $\nu_a(CH_2)$ frequency of **2** rose monotonically up to 2924 cm^{-1} at 130 °C, reaching a highly disordered state of the alkyl chains. The main phase transition took place in the range 60−80 °C, similar to the phase behavior of a glass transition, reflecting that the guanine moieties with the end-on orientation were predominantly stacked through $\pi-\pi$ interaction. Recent temperature-programmed desorption−mass spectroscopy studies indicate that the guanine molecules in the aggregated phase are stable at temperatures as high as 220 °C due to the strong cohesive interaction between them. The low thermal stability of the LB film of **2** suggests that the N7-substituted guanine moieties suppressed the formation of tetramers via cyclic interaction of hydrogen bonds. The $\nu_a(CH_2)$ frequencies of **1** and the equimolar mixture basically remained below 2918 cm^{-1} before 130 °C, with a slight increase above a temperature of 100 °C. It has been demonstrated that the intermolecular hydrogen bonding interaction between the headgroups can strengthen the interaction between the corresponding alkyl chains, so that the phase transition temperatures of the corresponding LB films are obviously enhanced.[54,55] In the case of **1**, the $\nu_a(CH_2)$ frequency showed a sudden increase from 2918 to 2923.5 cm^{-1} when the temperature was raised from 130 to 150 °C, indicative of an order−disorder phase behavior

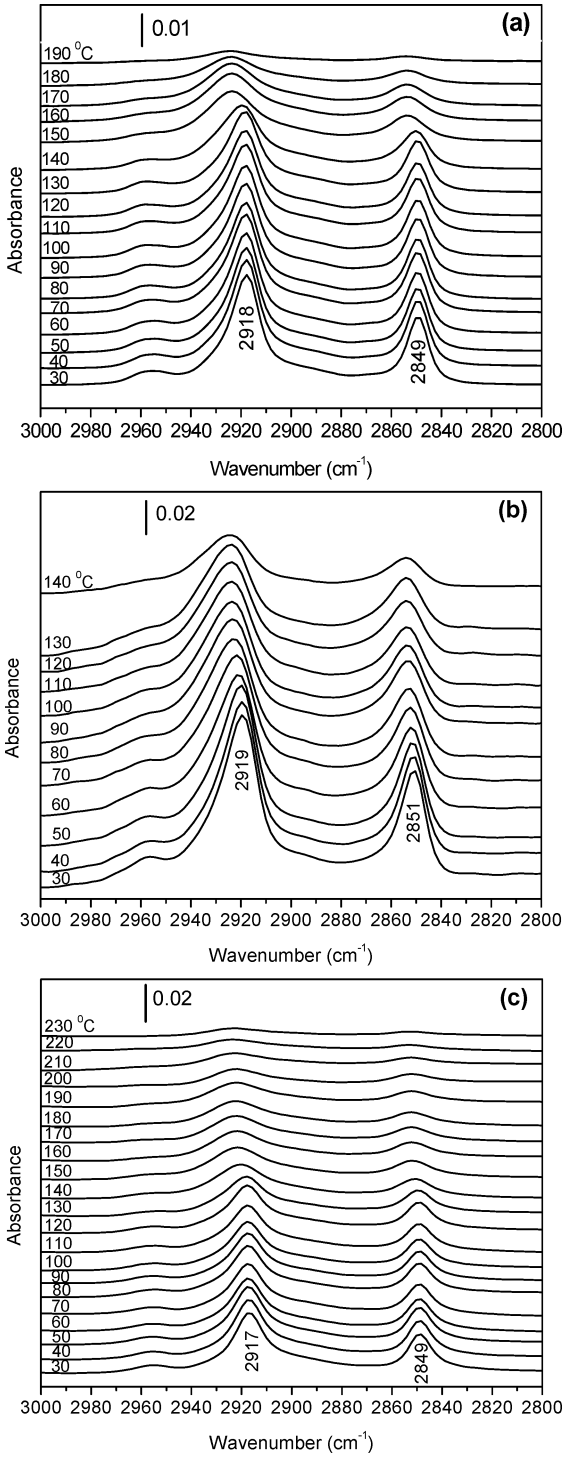

Figure 9. Variable-temperature FTIR transmission spectra of nine-layer LB films transferred from pure water in the region 3000−2800 cm^{-1}: (a) **1**; (b) **2**; (c) equimolar mixture.

of a typical crystal transition. This reflected the effect that the intermolecular hydrogen bonds between the adjacent cytosine moieties gave rise to an increase in the interaction between the alkyl chains.

For the equimolar mixture, the $\nu_a(CH_2)$ frequency was rapidly increased from ca. 2918 cm^{-1} at 130 °C to 2921.5 cm^{-1} at 150 °C and then remained almost unchanged within the range 2921.5−2922 cm^{-1} up to 200 °C. Upon further increase in temperature, the $\nu_a(CH_2)$ frequency rose to ca. 2923.5 cm^{-1}. It was obvious that the thermal stability of the LB film of the equimolar mixture was improved in comparison to those of the

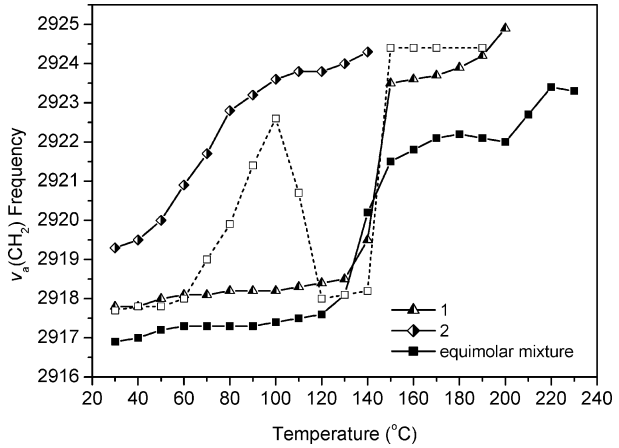

Figure 10. Temperature dependence of the antisymmetric CH_2 stretching frequencies for the nine-layer LB films of nucleolipids **1**, **2**, and their equimolar mixture transferred from pure water, together with the LB film of **1** from aqueous guanosine solution for comparison (□, ref 19).

two individual components. It was the triple hydrogen bonds of the specific molecular recognition between the complementary base moieties in the monolayers that strengthened the interaction between the corresponding alkyl chains. The phase transition behavior was also different from that of the LB film of **1** transferred from the aqueous guanosine subphase.[19] The hydrocarbon chains in the latter maintain ordered all-trans conformations prior to 60 °C.[19] When the temperature was elevated above 60 °C, the gauche conformers in the alkyl chains increased and the triple hydrogen bonding interaction started weakening; simultaneously, the hydrogen bond between the adjacent cytosine moieties in the monolayers was gradually formed.[19] When the temperature was increased to 120 °C, the intermolecular hydrogen bonds between the cytosine and guanosine base pairs were completely dissociated and the hydrogen bonded network between the adjacent cytosine moieties in the monolayers was formed. The almost all-trans conformations in the alkyl chains were recovered.[19] Although the intermolecular hydrogen bonding interaction between the cytosine and guanosine base pairs was stronger than that between the cytosine moieties in the monolayers,[19] the hydrogen bonding interaction between the base pairs after molecular recognition could strengthen neither the interaction between the hydrophilic headgroups of the nucleolipids nor the interaction between the corresponding hydrophobic chains. Therefore, only when the hydrogen bonding interaction strengthened the interaction between the headgroups of the nucleolipids could the strong hydrogen bonding interaction between the complementary bases induce an increase in the interaction between the corresponding alkyl chains, which will give a guide to the molecular design of amphiphiles for functional supramolecular architecture. The phase transition behaviors of the LB films of **1**, **2**, and their equimolar mixture provided powerful evidence for the specific molecular recognition of the cytosine and guanosine base pairs at the air−water interface through strong hydrogen-bonding interactions.

Conclusions

The studies of the IRRAS spectra and the isotherms of the monolayers of cytosine- and guanine-functionalized nucleolipids at the air−water interface indicated that the cytosine moieties in the monolayer of **1** were hydrogen bonded with an almost flat-on orientation and that the alkyl chains were uniaxially oriented with respect to the film normal. The guanine moieties in the monolayer of **2** were probably stacked through $\pi-\pi$ interaction with an end-on orientation, and the C−C−C planes of the alkyl chains were preferentially oriented parallel to the water surface. In the mixed monolayer of **1** and **2**, molecular recognition between the cytosine and guanine moieties occurred with the ring planes of base pairing and the C−C−C planes of the alkyl chains favorably oriented parallel to the water surface. The guanine moieties underwent an orientation change from an end-on mode prior to molecular recognition to a flat-on one after molecular recognition. Both the IRRAS spectra of the monolayers and the FTIR spectra of the LB films presented the exact sites in the cytosine and guanine moieties for the formation of triple hydrogen bonds. The base pairing resulted in a change in molecular orientation and interaction, and the corresponding LB film exhibited a different phase transition behavior from a typical crystal transition for **1** and an analogous glass transition for **2**. The thermal stability of the mixed LB film was improved in comparison to that of the LB films of pure components.

Acknowledgment. The authors are grateful to the reviewers for good suggestions. This work was supported by the Natural Science Foundation of China (Grant No. 20303008 and 20273029), the Ministry of Education, and Nanjing University.

Supporting Information Available: IRRAS spectra of the monolayers of nucleolipids **1**, **2**, and their equimolar mixture at the air−water interface at various angles of incidence. This material is available free of charge via the Internet at http://pub.acs.org.

References and Notes

(1) Lehn, J. M. *Supramolecular Chemistry*; VCH: Weinheim, 1995.
(2) Ringsdorf, H.; Schlarb, B.; Venzmer, J. *Angew. Chem., Int. Ed. Engl.* **1988**, *27*, 113.
(3) Piantadosi, C.; Marasco, C. J.; Morris-Natschke, S. L.; Meyer, K. L.; Gumus, F.; Surles, J. R.; Ishaq, K. S. *J. Med. Chem.* **1991**, *34*, 1408.
(4) Kimizuka, N.; Kawasaki, T.; Hirata, K.; Kunitake, T. *J. Am. Chem. Soc.* **1995**, *117*, 6360.
(5) Fersht, A. R. *Trends Biochem. Sci.* **1987**, *12*, 301.
(6) Ariga, K.; Kunitake, T. *Acc. Chem. Res.* **1998**, *31*, 371.
(7) Nowick, J. S.; Chen, J. S.; Noronda, G. *J. Am. Chem. Soc.* **1993**, *115*, 7636.
(8) Nowick, J. S.; Cao, T.; Noronda, G. *J. Am. Chem. Soc.* **1994**, *116*, 3285.
(9) Berti, D.; Barbaro, P.; Bucci, I.; Baglioni, P. *J. Phys. Chem. B* **1999**, *103*, 4916.
(10) Berti, D.; Baglioni, P.; Bonaccio, S.; Barsacchi-Bo, G.; Luisi, P. L. *J. Phys. Chem. B* **1998**, *102*, 303.
(11) Berndt, P.; Kurihara, K.; Kunitake, T. *Langmuir* **1995**, *11*, 3083.
(12) Berti, D.; Franchi, L.; Baglioni, P. *Langmuir* **1997**, *13*, 3438.
(13) Rädler, U.; Heiz, C.; Luisi, P. L.; Tampé, R. *Langmuir* **1998**, *14*, 6620.
(14) Ebara, Y.; Mizutani, K.; Okahata, Y. *Langmuir* **2000**, *16*, 2416.
(15) Huang, J.; Li, C.; Liang, Y. *Langmuir* **2000**, *16*, 3937.
(16) Li, C.; Huang, J.; Liang, Y. *Langmuir* **2000**, *16*, 7701.
(17) Li, C.; Huang, J.; Liang, Y. *Langmuir* **2001**, *17*, 2228.
(18) Shimomura, M.; Nakamura, F.; Ijiro, K.; Taketsuna, H.; Tanaka, M.; Nakamura, H.; Hasebe, K. *J. Am. Chem. Soc.* **1997**, *119*, 2341.
(19) Miao, W.; Du, X.; Liang, Y. *Langmuir* **2003**, *19*, 5398.
(20) Miao, W.; Du, X.; Liang, Y. *J. Phys. Chem. B* **2003**, *107*, 13636.
(21) Huo, Q.; Dziri, L.; Desbat, B.; Russell, K. C.; Leblanc, R. M. *J. Phys. Chem. B* **1999**, *103*, 2929.
(22) Kurihara, K.; Ohto, K.; Honda, Y.; Kunitake, T. *J. Am. Chem. Soc.* **1991**, *113*, 5077.
(23) Huo, Q.; Russell, K. C.; Leblanc, R. M. *Langmuir* **1998**, *14*, 2174.
(24) Koyano, H.; Yoshihara, K.; Ariga, K.; Kunitake, T.; Oishi, Y.; Kawano, O.; Kuramori, M.; Suehiro, K. *J. Chem. Soc., Chem. Commun.* **1996**, 1769.
(25) Pinnavaia, T. J.; Miles, H. T.; Becker, E. D. *J. Am. Chem. Soc.* **1975**, *97*, 7198.

(26) Pinnavaia, T. J.; Marshall, C. L.; Mettler, C. M.; Fisk, C. L.; Miles, H. T.; Becker, E. D. *J. Am. Chem. Soc.* **1978**, *100*, 3625.
(27) Dluhy, R. A.; Cornell, D. G. *J. Phys. Chem.* **1985**, *89*, 3195.
(28) Mendelsohn, R.; Braunder, J. W.; Gericke, A. *Ann. Rev. Phys. Chem.* **1995**, *46*, 305.
(29) Wada, T.; Inaki. Y.; Takemoto, K. *Polym. J.* **1989**, *21*, 11.
(30) Watson, J.; Crick, F. *Nature* **1953**, *171*, 737.
(31) Barker, D. L.; Marsh, R. E. *Acta Crystallogr.* **1964**, *17*, 1581
(32) Tao, N. J.; Shi, Z. *J. Phys. Chem.* **1994**, *98*, 1464.
(33) Broom, A. D.; Schweizer, M. P.; Ts'O, P. O. P. *J. Am. Chem. Soc.* **1967**, *89*, 3612.
(34) Tao, N. J.; DeRose, J. A.; Lindsay, S. M. *J. Phys. Chem.* **1993**, *97*, 910.
(35) Gaines, G. L., Jr. *Insoluble Monolayers at Liquid−Gas Interfaces*; Wiley-Interscience: New York, 1966.
(36) Ferreira, M.; Wohnrath, K.; Riul, A., Jr.; Giacometti, J. A.; Oliveira, O. N., Jr. *J. Phys. Chem. B* **2002**, *106*, 7272.
(37) Snyder, R. G.; Hsu, S. L.; Krimm, S. *Spectrochim. Acta* **1978**, *34A*, 395.
(38) Snyder, R. G.; Strauss, H. L.; Elliger, C. A. *J. Phys. Chem.* **1982**, *86*, 5145.
(39) Österblom, M.; Liedberg, B.; Demers, L. M.; Mirkin, C. A. *J. Phys. Chem. B* **2005**, *109*, 15150.
(40) Szczesniak, M.; Szczepaniak, K.; Kwiatkowski, J. S.; Kubulat, K.; Person, W. B. *J. Am. Chem. Soc.* **1988**, *110*, 8319.
(41) Lord, R. C.; Thomas, G. J., Jr. *Spectrochim. Acta* **1967**, *23A*, 2551.
(42) Florián, J.; Baumruk, V.; Leszczyñski, J. *J. Phys. Chem.* **1996**, *100*, 5578.
(43) Lin-Vien, D.; Colthup, N. B.; Fateley, W. G.; Grasselli, J. G. *The Handbook of Infrared and Raman Characteristic Frequencies of Organic Molecules*; Academic Press: San Diego, CA, 1991.
(44) Mathlouthi, M.; Seuvre, A. M. *Carbohydr. Res.* **1986**, *146*, 1.
(45) Szczepaniak, K.; Szczesniak, M. *J. Mol. Struct.* **1987**, *156*, 29.
(46) Snyder, R. G. *J. Mol. Spectrosc.* **1961**, *7*, 116.
(47) Bertie, J. E.; Ahmed, M. K.; Eysel, H. H. *J. Phys. Chem.* **1989**, *93*, 2210.
(48) Kuzmin, V. L.; Michailov, A. V. *Opt. Spectrosc.* **1981**, *51*, 383.
(49) Gericke, A.; Kerth, A.; Blume, A. *Infrared Spectroscopic Investigation of Lipid and Protein Monolayers at the Air/Water Interface*. Bio-Medical FT-IR/NIR/Raman application. http://www.bruker.com/optics (accessed Sept 2003).
(50) Du, X.; Miao, W.; Liang, Y. *J. Phys. Chem. B* **2005**, *109*, 7428.
(51) Tasumi, M.; Shimanouchi, T. *J. Chem. Phys.* **1965**, *43*, 124.
(52) Holland, R. F.; Nielsen, J. R.; *J. Mol. Spectrosc.* **1962**, *8*, 383.
(53) Holland, R. F.; Nielsen, J. R.; *J. Mol. Spectrosc.* **1962**, *9*, 436.
(54) Du, X.; Shi, B.; Liang, Y. *Langmuir* **1998**, *14*, 3631.
(55) Du, X.; Liang, Y. *J. Phys. Chem. B* **2000**, *104*, 10047.